In-Line and Transverse Forces on Cylinders in Oscillatory Flow at High Reynolds Numbers.

By

Turgut Sarpkaya, Naval Postgraduate School

ABSTRACT

This paper presents the results of an extensive experimental investigation of the in-line and transverse forces acting on smooth and rough circular cylinders placed in oscillatory flow at Reynolds numbers up to 700,000, Keulegan-Carpenter numbers up to 150, and relative roughnesses from 0.002 to 0.02. The drag and inertia coefficients have been determined through the use of the Fourier analysis and the least squares method. The transverse force (lift) has been analysed in terms of its maximum, semi peak-to-peak, and root-mean-square values. In addition, the frequency of vortex shedding and the Strouhal number have been determined.

The results have shown that (a) for smooth cylinders, all of the coefficients cited above are functions of the Reynolds and Keulegan and Carpenter numbers, particularly for Reynolds numbers larger than about 20,000; (b) for rough cylinders, the force coefficients also depend on the relative roughness k/D and differ significantly from those corresponding to the smooth cylinder; and that (c) the use of the 'frequency parameter' $D^2/\nu T$ and the roughness Reynolds number $U_m k/\nu$ allow a new interpretation of the present as well as the previously obtained data and the establishment of model laws for oscillatory flow about cylinders at supercritical Reynolds numbers.

References and illustrations at end of paper.

INTRODUCTION

The design of structures for the marine environment requires the prediction of the forces generated by waves and currents. Much of the present knowledge has been obtained by means of model tests at Reynolds numbers generally two to three orders of magnitude smaller than prototype Reynolds numbers. These model tests have relied heavily on the so-called Morison formula for expressing the force as the sum of a drag and inertia force. The values of the drag and inertia coefficients to be used in the Morison equation became the subject of many experimental studies in the last twenty years. The correlation of these coefficients with the relative amplitude of the waves (or the Keulegan-Carpenter number) has been generally inconclusive. Furthermore, lift forces which are associated with vortex shedding have received relatively little attention. It thus became clear that much is to be gained by considering plane oscillatory flow about cylinders at high Reynolds numbers in order to isolate the influence of individual factors such as relative amplitude, Reynolds number, and the relative roughness on vortex shedding and resistance. It is with this realization that the present investigation was undertaken and the preliminary results obtained with

smooth cylinders in a small U-shaped water tunnel operating at relatively low Reynolds numbers (2,500 to 25,000) have been previously reported [1].

The present paper deals with in-line and transverse forces acting on smooth and artificially-roughened circular cylinders in harmonic flow at critical and supercritical Reynolds numbers.

APPARATUS AND PROCEDURE

Of the two possible methods of generating relative harmonic fluid motion about bluff bodies, namely, oscillating the fluid or the body, the former has been chosen. The relative merits and shortcomings of the two methods have been amply discussed [2] and will not be repeated here. Suffice it to note that large amplitude structural and free surface oscillations commonly encountered in oscillating the body in a fluid otherwise at rest do not lead to reliable data. The advantages of the apparatus used herein for the purpose under consideration have already been demonstrated [1] and will become further evident from the data to be presented.

The oscillating flow system consisted of a large U-shaped vertical water tunnel as shown in Fig. 1. The cross-section of the two vertical legs is 3 ft by 6 ft and that of the test section is 3 ft by 3 ft. The two corners of the tunnel were carefully streamlined to prevent flow separation. This design proved to be more than adequate for no separation was encountered, and also the desired frequency and amplitude of oscillation were achieved. The auxiliary components of the tunnel consisted of plumbing for hot and cold water, butterfly-valve system, and the air-supply system.

The butterfly-valve system (mounted on top of one of the legs of the tunnel) consisted of four plates, each 18 inches wide and 36 inches long. All four valves were simultaneously driven by a simple rack and pinion system actuated by an air-driven piston and a three-way pneumatic valve. Initially, the butterfly valves were closed and air was introduced to that side of the tunnel, with an electrically-controlled ball valve, to create the desired differential water level between the two legs of the tunnel. Then the valves were opened with the help of the rack and pinion system and the three-way control valve. This action set the fluid in the tunnel in oscillatory motion with a natural period of T = 5.272 seconds. The elevation, acceleration, and all force traces were absolutely free from secondary oscillations so that no filters whatsoever were used between the outputs of the transducers and the recording equipment (see Fig. 2).

Throughout the investigation, the monitoring of the characteristics of the oscillations in the tunnel was of prime importance in view of the fact that most of the difficulties in the past in the determination of the drag, lift, and inertia coefficients resulted from the difficulty of generating a purely harmonic motion free from vibrations or from applying theoretically derived rather than measured values for velocities and accelerations.

Three transducers were used to generate three independent d.c. signals, each proportional to the instantaneous value of elevation, velocity and acceleration. The first one consisted of a platinum wire stretched vertically in one leg of the tunnel. The response of the wire was perfectly linear within the range of oscillations encountered. The second method consisted of the measurement of the instantaneous acceleration by means of a differential-pressure transducer connected to two pressure taps placed horizontally 2 ft apart and 4 ft to one side of the test section. The instantaneous acceleration was then calculated from $\Delta p = \rho s \cdot dU/dt$ where Δp is the differential pressure, s the distance between the pressure taps and dU/dt is the instantaneous acceleration of the fluid. The third method again consisted of the measurement of the differential pressure between two pressure taps placed symmetrically on the two vertical legs of the tunnel at an elevation H ft below the mean water level. The linear differential-pressure transducer yielded the instantaneous elevation and hence the amplitude of oscillation since, according to Bernoulli's equation

$$A = 2A_0 = [\Delta p/\gamma]_{max}/[1 - (2\pi/T)^2 H/g] \qquad (1)$$

in which g and T are constant and H is kept constant.

All three methods gave nearly identical results and yielded the amplitude A, the maximum velocity $U_m = 2\pi A/T$, or the maximum acceleration $a_m = (2\pi/T)^2 A$ to an accuracy of about 2% relative to each other.

The in-line and transverse forces were measured with two identical, cantilever type, force transducers, one at each end of the cylinder. The gages had a capacity of 250 lbs and the deflection of the cantilever end was less than 0.008 inches. A special housing was built for each gage so that it can be mounted on the tunnel window and rotated to measure either the in-line or the transverse force alone. The test cylinders were placed in the test section by retracting the gages from their housing and then pushing them into the bearings mounted on each end of the cylinders. This allowed a gap of 1/32 inch between the cylinder and the tunnel wall. The natural frequency of the cylinder and force-transducer combination in water was about 20 times larger than the frequency of oscillation of the water column and about 10 times larger than the largest frequency of vortex shedding.

Seven circular cylinders with diameters ranging in size from 2 inches to 6.5 inches were used. The cylinders were turned on a lathe from aluminum pipes or plexiglass rods and polished to a mirror-shine surface. Same cylinders were also used as rough cylinders. For this purpose, sand was sieved to obtain the desired relative roughness and applied uniformly on the cylinder surface with an air-drying epoxy paint. After a series of tests with water at various temperatures, the cylinders were polished again and covered with sand of different size. This procedure was continued until the desired ranges of all the governing parameters were covered. The use of hot water increased the range of the Reynolds number by as much as 100%.

Experiments were repeated at least four times for each cylinder and for all suitably selected amplitudes, roughness hights, and water temperatures. The in-line and transverse forces were read every 0.1 second from the traces for the period of T = 5.272 seconds. Then the drag, inertia, and the lift coefficients, the vortex shedding frequency, Strouhal number, maximum error between the measured and calculated forces, etc. were evaluated through the use of the appropriate equations and a computer.

FORCE COEFFICIENTS AND GOVERNING PARAMETERS

Data reduction for the forces in-line with the direction of oscillation is based on Morison equation [3] and three different analysis of the force records, namely, Fourier analysis, least squares, and a modified least squares method.

The in-line force which consists of the drag force F_d and the inertia force F_i is assumed to be given by [3]

$$F=F_d+F_i=0.5C_d LD\rho|U|U +0.25C_m LD^2\pi\rho.dU/dt \qquad (2)$$

in which C_d and C_m represent respectively the drag and inertia coefficients and U the instantaneous velocity of the ambient flow. For an oscillating flow represented by $U=-U_m\cos\theta$, with $\theta=2\pi t/T$, the Fourier averages of C_d and C_m are given by Keulegan and Carpenter as [4]

$$C_d= -0.75 \int_0^{2\pi} (F_m\cos\theta/\rho U_m^2 LD)d\theta \qquad (3)$$

and

$$C_m= (2U_m T/\pi^3 D) \int_0^{2\pi} (F_m\sin\theta/\rho U_m^2 LD)d\theta \qquad (4)$$

in which F_m represents the measured force.

The method of least squares consists of the minimization of the error between the measured and calculated forces. This procedure yields [5]

$$C_{dls}= -(8/3\pi)\int_0^{2\pi} (F_m|\cos\theta|\cos\theta/\rho DLU_m^2)d\theta \qquad (5)$$

and $C_{mls}=C_m$. Evidently, the Fourier analysis and the method of least squares yield identical C_m values and that the C_d values differ only slightly. The details of the modified least-squares method may be found in Ref. [5] and will not be repeated here.

The transverse force has been expressed in terms of various coefficients. Some of these are (a) the maximum lift coefficient defined by $C_L=$ (maximum amplitude of the transverse force in a cycle)/$(0.5LD\rho U_m^2)$; (b) the semi peak-to-peak value of the transverse force normalized by $0.5LD\rho U_m^2$; and (c) the normalized root-mean-square value of the transverse force. In addition, the frequency of the oscillations of the transverse force and the Strouhal number have been evaluated.

It is recognized that the coefficients cited above are not constant throughout the cycle and are either time-invariant averages or peak values at a particular moment in the cycle. A simple dimensional analysis of the flow under consideration shows that the time-dependent coefficients may be written as

$$F/(0.5DL\rho U_m^2)= f(U_m T/D, U_m D/\nu, k/D, t/T) \qquad (6)$$

in which F represents the in-line or the transverse force. Equation (6), combined with Eq. (2), assuming for now that the latter is indeed valid, yields

$$C_d= f_1(K, Re, k/D, t/T) \qquad (7)$$

$$C_m= f_2(K, Re, k/D, t/T) \qquad (8)$$

in which $K = U_m T/D$ and $Re = U_m D/\nu$, and k/D represents the relative roughness.

There is no simple way to deal with Eqs. (7) and (8) even for the most manageable time-dependent flows. Another and perhaps the only other alternative is to eliminate time as an independent variable and consider suitable time-invariant averages as given by Eqs. (3), (4), and (5). Thus, one has

$$\begin{Bmatrix} C_d \\ C_m \\ C_L \\ \vdots \end{Bmatrix} = f_i(K, Re, k/D) \qquad (9)$$

It appears, for the purposes of Eq. (9), that the Reynolds number is not the most suitable parameter involving viscosity. The primary reasons for this are that the effect of viscosity is relatively small and that U_m appears in both K and Re. Thus, replacing Re by $Re/K = D^2/\nu T$ in Eq. (9), one has

$$C_i(a coefficient) = f_i(K, \beta, k/D) \qquad (10)$$

in which $\beta = D^2/\nu T$ and shall be called the

'frequency parameter'. Evidently, β is constant for a series of experiments conducted with a cylinder of diameter D in water of uniform and constant temperature since T is constant. Then the variation of a force coefficient with K may be plotted for constant values of β. Subsequently, one can easily recover the Reynolds number from Re = Kβ and connect the points, on each β=constant curve, representing a given Re.

Let us now re-examine a set of data previously obtained by others [4] partly to illustrate the use and significance of β as one of the governing parameters and partly to take up the question of the effect of Reynolds number on the force coefficients.

The data given by Keulegan and Carpenter [4] may be represented by 12 different values of β. The drag and inertia coefficients are plotted in Figs. 3 and 4 and connected with straightline segments. Evidently, the identification of the individual data points in terms of the cylinder diameter, as was done by Keulegan and Carpenter [4] and also by Sarpkaya [1], irrespective of the β values gives the impression of a scatter in the data and invites one to draw a mean drag curve through all data points. Such a temptation is further increased by the fact that the data for each β span over only a small range of K values. Evidently, the drawing of such a mean curve eliminates the dependence of C_d and/or C_m on β and hence on Re.

Also shown in Figs. 3 and 4 are points representing four selected Reynolds numbers. The corresponding K values for each Re and β were calculated from K = Re/β. The points corresponding to the selected Reynolds numbers are reproduced in Figs. 5 and 6. These figures show, within the range of Re and K values encountered in Keulegan-Carpenter data, that (a) C_d depends on both K and Re and decreases with increasing Re for a given K; and that (b) C_m depends on both K and Re for K larger than approximately 15 and decreases with increasing Re. A similar analysis of Sarpkaya's data [1] also shows that C_d and C_m depend on both K and Re and that C_m increases with increasing Re. Notwithstanding this difference in the variation of C_m between the two sets of data, Figs. 5 and 6 put to rest the long standing controversy regarding the dependence or lack of dependence of C_d and C_m on Re and show the importance of β as one of the governing parameters in interpreting the data, in interpolating the K values for a given Re, and in providing guide lines for further experiments as far as the ranges of K and β are concerned.

RESULTS AND DISCUSSIONS

Drag and Inertia Coefficients for Smooth and Rough Cylinders - Only the representative data will be presented herein for sake of brevity.

The tabulated as well as plotted data for all force coefficients are given in Ref. [2].

Figures 7 and 8 show C_d versus K and C_m versus K for five values of β. Evidently, there is very little scatter in the data even though the figures represent the results of four independent runs. A summary of the complete data for all cylinders is presented in Figs. 9 and 10. Also shown in Figs. 9 and 10 are the constant Re lines obtained through the use of K = Re/β. Evidently, there is a remarkable correlation between the force coefficients, Reynolds number, and the Keulegan-Carpenter number. The smoothness of the constant Re lines is another indication of the consistency of the data from one cylinder to another.

Figures 9 and 10 show that C_d and C_m do not vary appreciably with Re for Re smaller than about 20,000 and help to explain the conclusions previously reached by Keulegan and Carpenter [4] and Sarpkaya [1].

The data, similar to those given in Figs. 7 through 10, are also plotted as a function of Re for constant values of K in Figs. 11 and 12 since it is believed that the Reynolds number is the liveliest of all the non-dimensional parameters. These figures clearly show that C_d decreases with increasing Re to a value of about 0.5 (dependent on K) and then begins to increase with further increase in Re. The inertia coefficient C_m increases with increasing Re, reaches a maximum, and then gradually approaches a value of about 1.75. It will be recalled that the Keulegan-Carpenter data indicated an opposite trend. It is believed that the Keulegan-Carpenter data for C_m are not quite reliable for K > 15. This is also evident from the observation that the data corresponding to β=141 appear to be out of place (see Fig. 4) relative to those corresponding to β=97 and 217. Suffice it to say that the results presented in Figs. 7 through 12 shed new light on the variations of the drag and inertia coefficients and partly explain the reasons for the large scatter encountered in the plots of C_d versus Re and C_m versus Re as compiled by Wiegel [6].

The data obtained with artificially-roughened cylinders are presented in Figs. 13 and 14 in a manner similar to those given in Figs. 11 and 12. It must be noted that there exists two such figures for every value of K. However, the results shown in Figs. 13 and 14 did not appreciably vary with K for 30 < K < 60 (see also Fig. 11).

Figures 13 and 14 show that the effect of roughness on the resistance to harmonic flow is quite significant. Not only the presence of vortices on both sides of the cylinder and the increased level of turbulence but also the roughness bring about an earlier transition to

turbulence. Following the transition of the entire boundary layer to turbulence during most of the cycle, the flow reaches a supercritical state and both the drag and inertia coefficients acquire nearly constant values. Even though the actual events are somewhat more complicated, it seems unlikely that there will be any further transitions in the boundary layer.

The reason for the experiments with rough cylinders is of course more than the desire to examine the effect of relative roughness on C_d, C_m, and C_L. It is prompted essentially by an attempt at artificially increasing the Reynolds number to supercritical regime by means of surface roughness. Recent experiments [7, 8] with steady flow over rough cylinders have shown that (a) a change in flow regime takes place at a Reynolds number Vk/ν of about 200 independently of the diametral Reynolds number; (b) a correct surface roughness condition provokes supercritical flow for $Vk/\nu > 200$, (the condition that must be respected is $k/D < 0.0022$); (c) a smooth cylinder is not a special case but behaves as if it had a roughness of $k/D = 0.000035$; and that (d) the apparent diametral Reynolds number is increased by a factor $k/(0.000035.D)$ for a cylinder of diameter D and surface roughness k. The importance and the consequences of these conclusions are self evident for supercritical Reynolds number simulation for flow over circular cylinders.

In order to carry over the above ideas to harmonic flow, the data given in Fig. 13 were replotted in Fig. 15 as a function of $U_m k/\nu$ for various values of k/D. A similar plot for C_m has been prepared but will not be presented here due to space limitations. Also shown in Fig. 15 are the mean lines corresponding to steady flow as compiled by Szechenyi [7]. Figure 15 shows that a change in the flow regime takes place at a roughness Reynolds number of about 130 and that the drag coefficient approaches values between 0.9 and 1.0 for $k/D < 0.002$. Evidently, the change in the flow regime occurs at higher values of $U_m k/\nu$ with increasing k/D. Of special interest for simulation purposes, however, is the smaller relative roughness.

The magnitude of the apparent increase in the diametral Reynolds number can be estimated by fitting the curve obtained for smooth cylinders (see Figs. 11 and 13) for K = 50 onto the rough cylinder results shown in Fig. 15. Working back from the resulting values of $U_m k/\nu$ on the abscissa, this procedure gives an effective relative roughness between 0.0004 and 0.0006 for the smooth cylinder in harmonic flow with K = 50. Further exploration of these ideas will be extremely important in model tests and in the simulation of supercritical Reynolds numbers. It must, however, be kept in mind that the actual events in harmonic flow are considerably more complicated and that the effect of roughness

cannot be represented by k/D alone. Additional parameters such as the size distribution, shape and packing of grains must be introduced. Alternatively, one can define an equivalent roughness height k_s [9] or a roughness-length parameter based on the actual boundary-layer characteristics.

Transverse Force and Vortex Shedding for Smooth and Rough Cylinders - The data for the maximum lift coefficient for smooth cylinders are summarized in Figs. 16 and 17. The original data in plotted and tabulated form are presented in Ref. [2]. Evidently, the lift coefficient depends on Re for Re larger than about 20,000 and rapidly decreases to about 0.2 for larger values of Re and K. It is also evident that the lift force is a major portion of the total force acting on the cylinder and cannot be neglected in the design of structures.

The frequency of the alternating transverse force is shown in Fig. 18 in terms of $f_r = f_v/f$ as a function of K and Re. It is apparent that f_r is not constant and increases with increasing K and Re. Furthermore, a quick calculation through the use of Fig. 18 shows that the Strouhal number given by $f_v D/U_m = f_r/K$ is not constant at 0.2, as in steady flow, and depends on both Re and K. Experiments with rough cylinders yielded similar results for C_L, f_r, and the Strouhal number [2]. Largest lift as well as the largest in-line force tended to occur at the time of maximum velocity. This in turn decreased the phase angle and hence the inertia coefficient and increased the drag coefficient relative to smooth cylinder. Thus, roughness increases the maximum instantaneous force acting on the cylinder by synchronizing the occurrence of the maximum in-line and transverse forces at or near the time of maximum velocity.

CONCLUSIONS

The results presented herein warrant the following conclusions: (a) For smooth cylinders, the drag, lift, and the inertia coefficients depend on both the Reynolds and Keulegan and Carpenter numbers; (b) For rough cylinders, the same force coefficients become independent of the Reynolds number above a critical value and depend only on the Keulegan and Carpenter number and the relative roughness; (c) Correct artificial roughness may be used to provoke and simulate supercritical flow in model tests in steady as well as oscillatory flows; (d) For both smooth and rough cylinders, the relationship between the drag and inertia coefficients is not unique and depends on the particular value of the Keulegan and Carpenter number; (e) The transverse force is a significant fraction of the total resistance at all Reynolds numbers and must be considered in the design of structures; (f) The frequency of the shedding of the primary vortices increases at more or less discrete steps with

increasing Reynolds and Keulegan-Carpenter numbers; (g) The results reported herein and the conclusions arrived at are applicable only to cylinders in harmonic flow with zero mean velocity. The force coefficients for harmonic flow with a mean velocity superimposed on it may differ significantly from those reported herein; and finally, (h) it is hoped that the data presented herein will accentuate the need for actual full scale experiments and enable those concerned to interpret and better understand the factors effecting the force-transfer coefficients in wavy flows.

NOMENCLATURE

A	Amplitude of oscillations at the test section
A_o	Amplitude of oscillations at the free surface
C_d	Drag coefficient
C_L	Maximum lift coefficient
C_m	Inertia coefficient
D	Diameter of the test cylinder
F	Force
F_d	Drag force
F_i	Inertial force
f	Frequency of oscillations, 1/T
f_v	Frequency of vortex shedding (first harmonic)
g	Gravitational acceleration
H	Elevation (see Fig. 1)
K	Keulegan-Carpenter number, $U_m T/D$
k	Roughness height
L	Length of the test cylinder
p	Pressure
Re	Reynolds number, $U_m D/\nu$
T	Period of oscillations in the tunnel
t	time
U	Instantaneous velocity
U_m	Maximum velocity in the cycle
V	Velocity in steady flow
β	Frequency parameter, $D^2/\nu T$
γ	Specific weight of water
θ	$2\pi t/T$
ν	Kinematic viscosity of water
ρ	Density of water

ACKNOWLEDGMENT

REFERENCES

1. Sarpkaya, T.:"Forces on Cylinders and Spheres in a Sinusoidally Oscillating Fluid", Journal of Applied Mechanics, ASME, Vol. 42, No. 1, March 1975, pp. 32-37.

2. Sarpkaya, T.:"Vortex Shedding and Resistance in Harmonic Flow About Smooth and Rough Circular Cylinders at High Reynolds Numbers", Naval Postgraduate School Technical Report No. NPS-59SL76021, February 1976, Monterey, California.

3. Morison, J. R., et al.:"The Force Exerted by Surface Waves on Piles", Petroleum Trans., Vol. 189, 1950, pp. 149-157.

4. Keulegan, G. H. and Carpenter, L. H.:"Forces on Cylinders and Plates in an Oscillating Fluid", Journal of Research of the National Bureau of Standards, Research Paper No. 2857, Vol. 60, No. 5, May 1958.

5. Sarpkaya, T.:"Forces on Cylinders Near a Plane Boundary in a Sinusoidally Oscillating Fluid", Fluid Mechanics in the Petroleum Industry, ASME, December 1975, pp. 43-47.

6. Wiegel, R. L.: Oceanographical Engineering, Prentice Hall, Inc., Englewood Cliffs, N. J., 1964, pp. 257-260.

7. Szechenyi, E.:"Supercritical Reynolds Number Simulation for Two-Dimensional Flow Over Circular Cylinders", Journal of Fluid Mechanics, Vol. 70, Part 3, 1975, pp. 529-542.

8. Guven, O., Patel, V. C., and Farell, C.: "Surface Roughness Effects on the Mean Flow Past Circular Cylinders", Iowa Institute of Hydraulic Research Report No. 175, May 1975, Iowa City, Iowa.

9. Schlichting, H.: Boundary-Layer Theory, McGraw-Hill Book Co., N. Y., 1968, (6-th ed.), pp. 578-586.
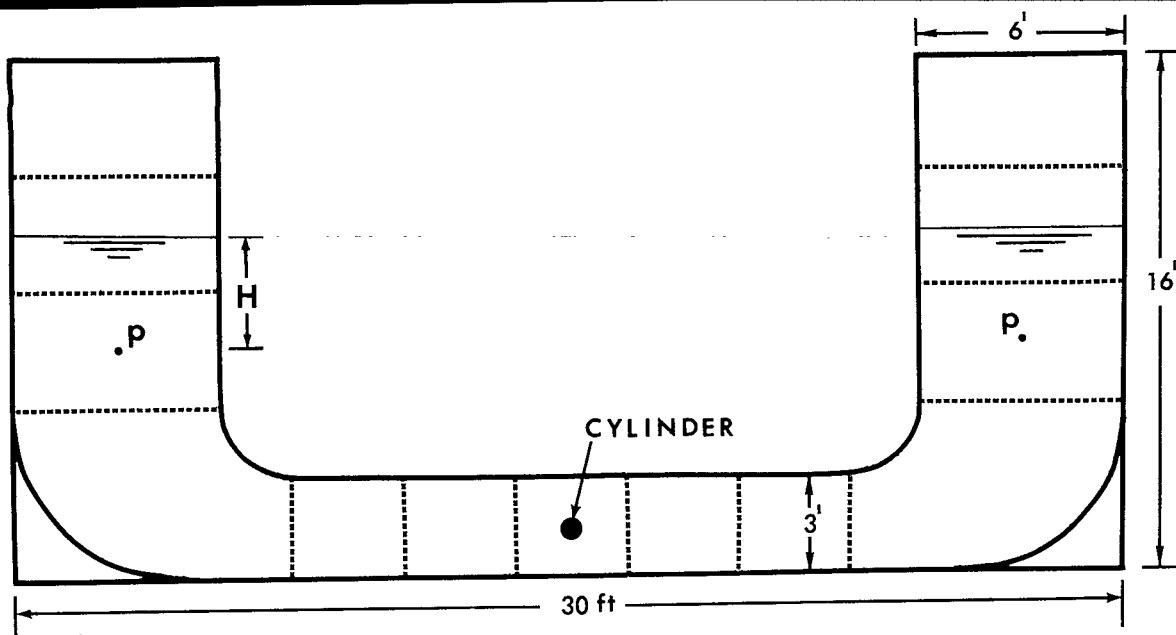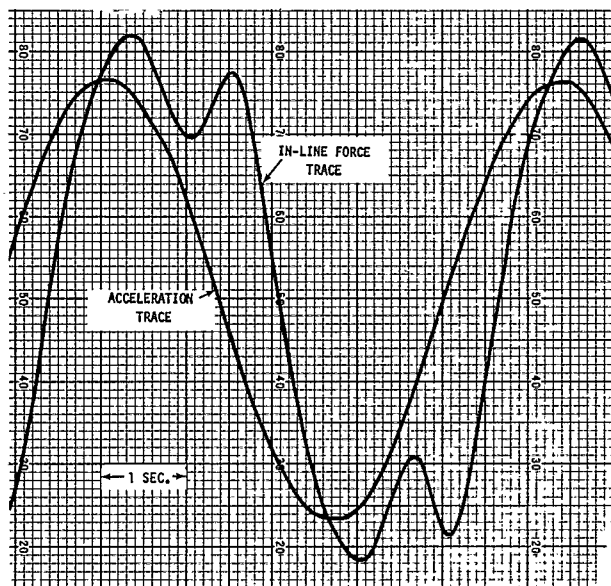
FIG. 1 – THE U-SHAPED VERTICAL WATER TUNNEL.

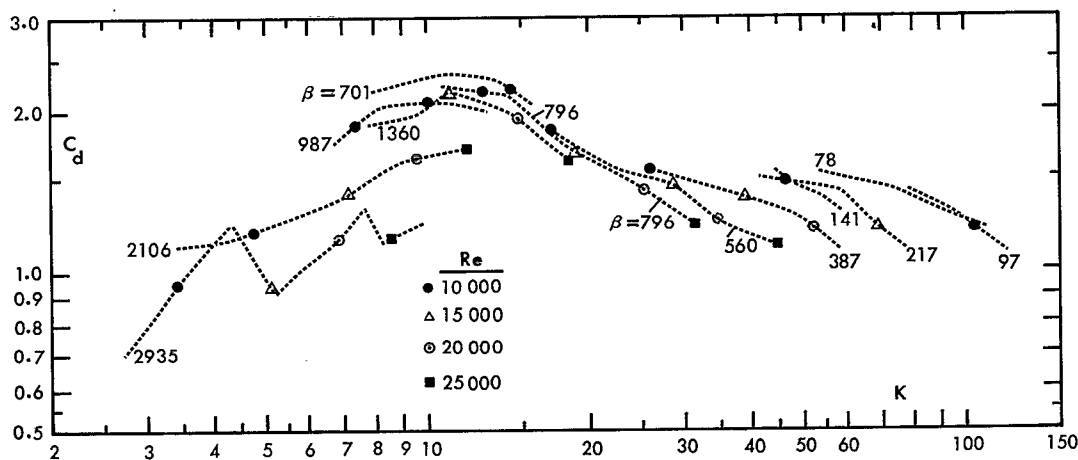FIG. 2 – SAMPLE FORCE AND
ACCELERATION TRACES.

FIG. 3 - DRAG COEFFICIENT VS THE KEULEGAN-CARPENTER NUMBER FOR THE
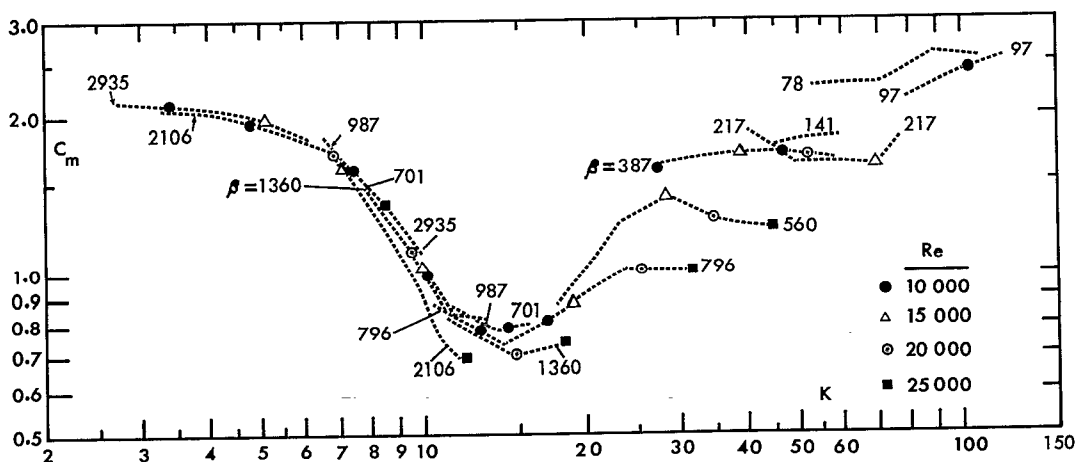KEULEGAN-CARPENTER DATA FOR CONSTANT VALUES OF THE FREQUENCY
PARAMETER.

FIG. 4 - INERTIA COEFFICIENT VS THE KEULEGAN-CARPENTER NUMBER FOR
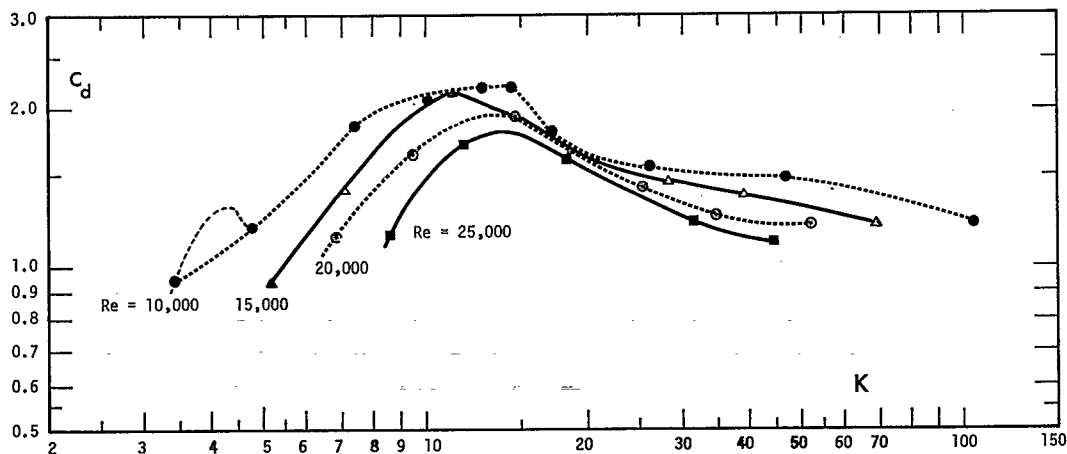THE KEULEGAN-CARPENTER DATA FOR CONSTANT VALUES OF THE FREQUENCY
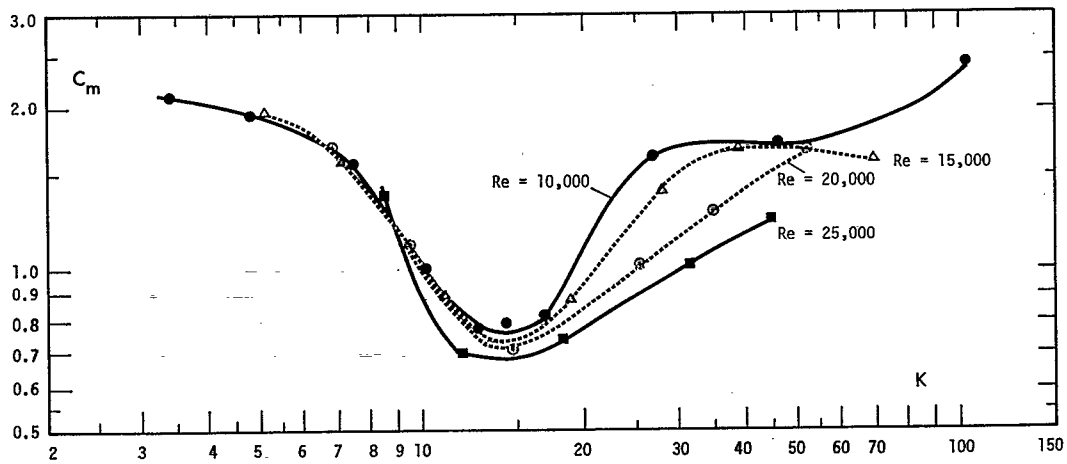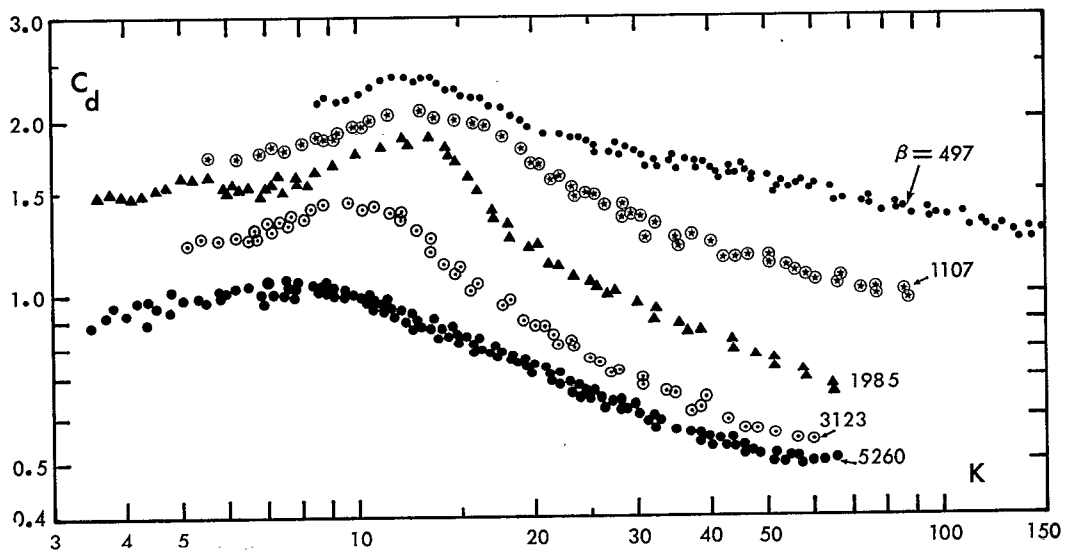PARAMETER

FIG. 5 - DRAG COEFFICIENT VS THE KEULEGAN-CARPENTER NUMBER FOR
THE KEULEGAN-CARPENTER DATA FOR CONSTANT REYNOLDS NUMBERS.

FIG. 6 – INERTIA COEFFICIENT VS THE KEULEGAN-CARPENTER NUMBER
FOR THE KEULEGAN-CARPENTER DATA FOR CONSTANT REYNOLDS NUMBERS.

FIG. 7 – DRAG COEFFICIENT VS THE KEULEGAN-CARPENTER NUMBER FOR
CONSTANT VALUES OF THE FREQUENCY PARAMETER (PRESENT DATA).
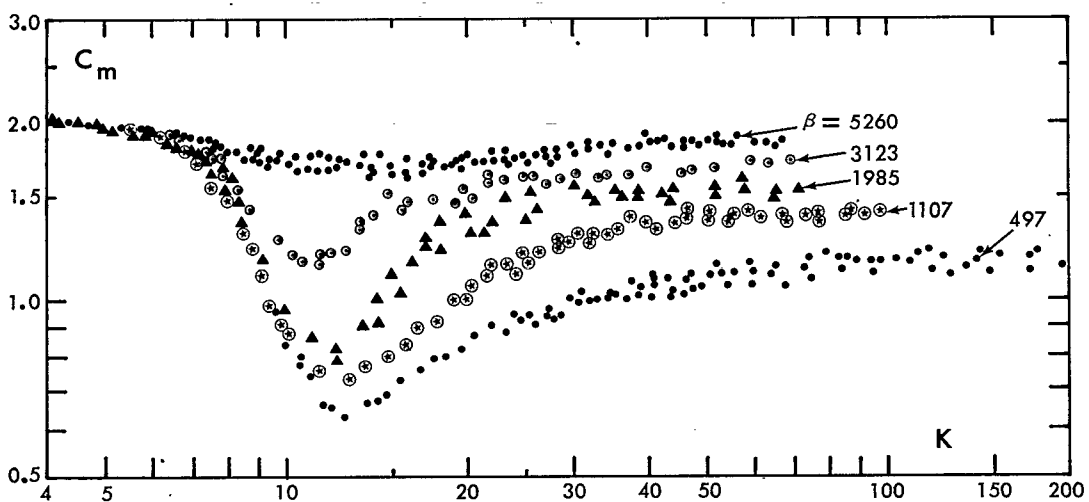
FIG. 8 – INERTIA COEFFICIENT VS THE KEULEGAN-CARPENTER NUMBER FOR
CONSTANT VALUES OF THE FREQUENCY PARAMETER (PRESENT DATA).
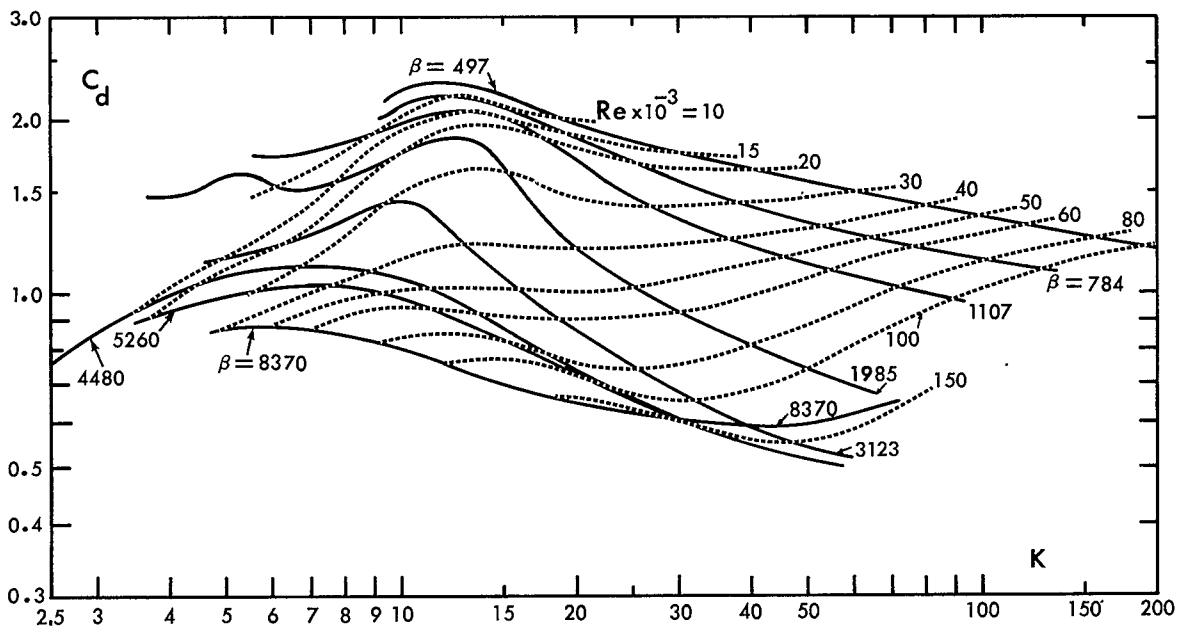
FIG. 9 – DRAG COEFFICIENT VS THE KEULEGAN-CARPENTER NUMBER FOR
CONSTANT VALUES OF THE FREQUENCY PARAMETER AND THE REYNOLDS
NUMBER.
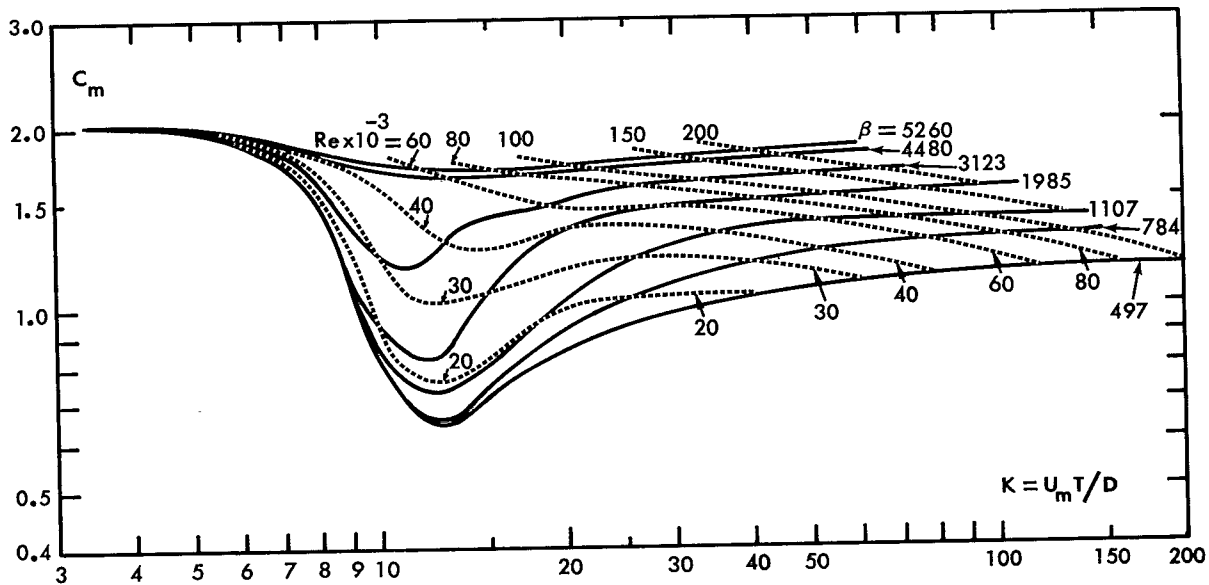
FIG. 10 – INERTIA COEFFICIENT VS THE KEULEGAN-CARPENTER NUMBER
FOR CONSTANT VALUES OF THE FREQUENCY PARAMETER AND THE REYNOLDS
NUMBER.
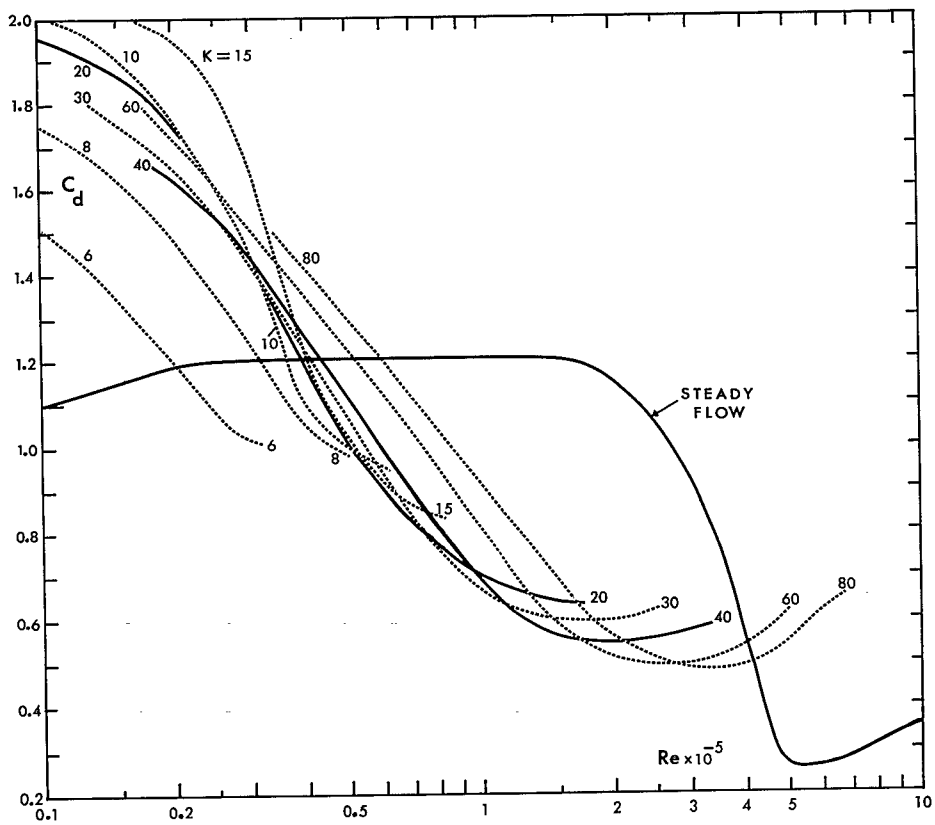
FIG. 11 – DRAG COEFFICIENT VS REYNOLDS NUMBER FOR CONSTANT VALUES OF K.
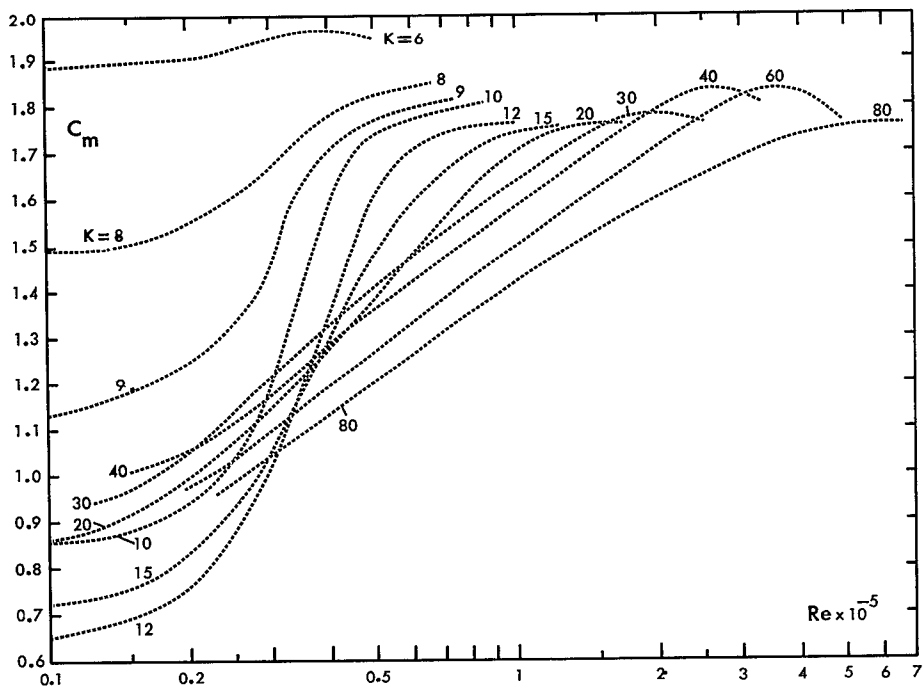
FIG. 12 – INERTIA COEFFICIENT VS REYNOLDS NUMBER FOR CONSTANT VALUES OF K.
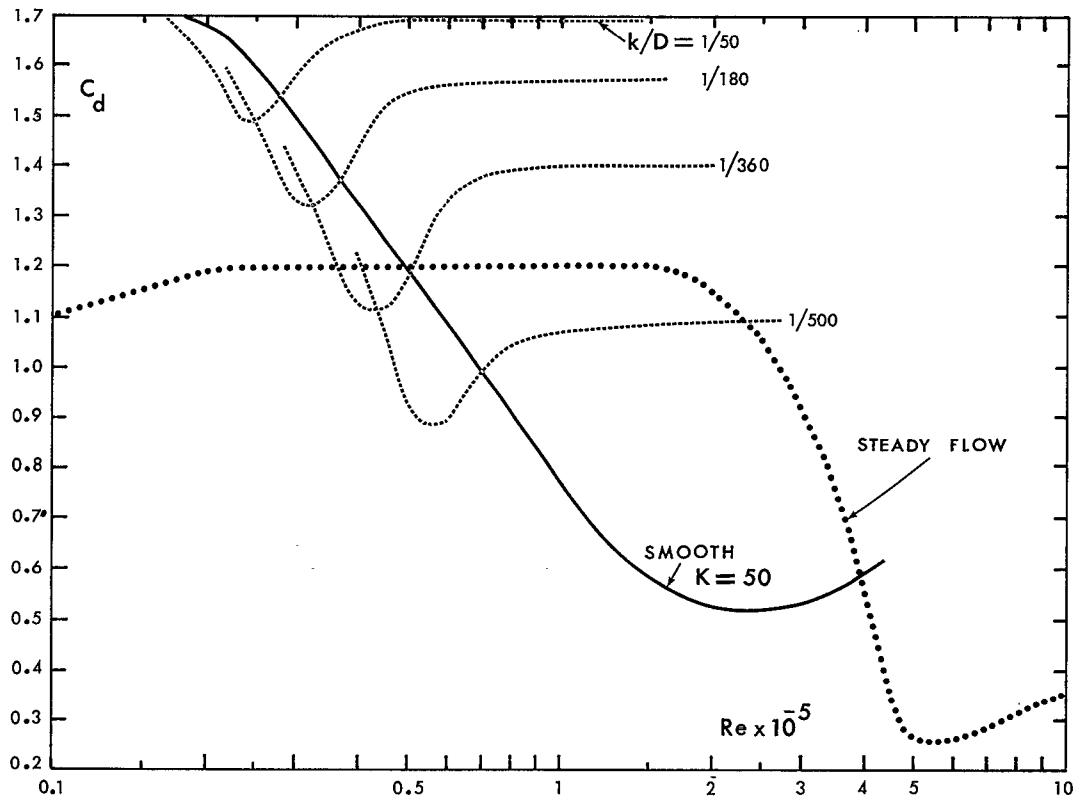
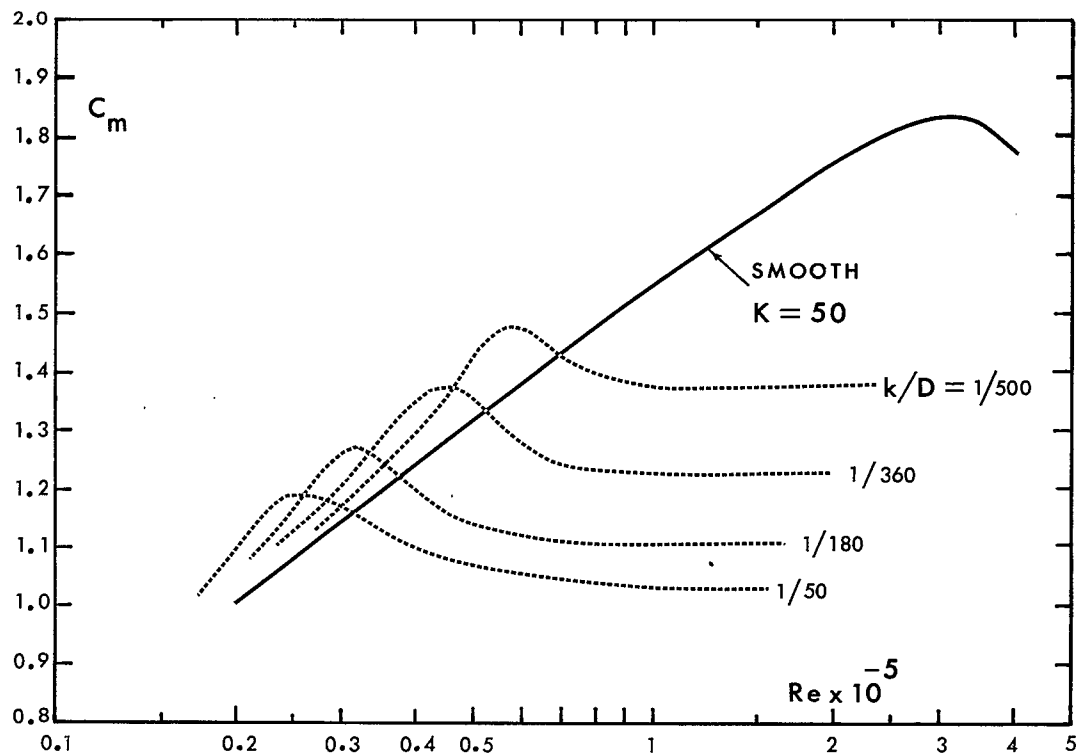FIG. 13 - DRAG COEFFICIENT VS REYNOLDS NUMBER FOR ROUGH CYLINDERS.

FIG. 14 - INERTIA COEFFICIENT VS REYNOLDS NUMBER FOR ROUGH CYLINDERS.
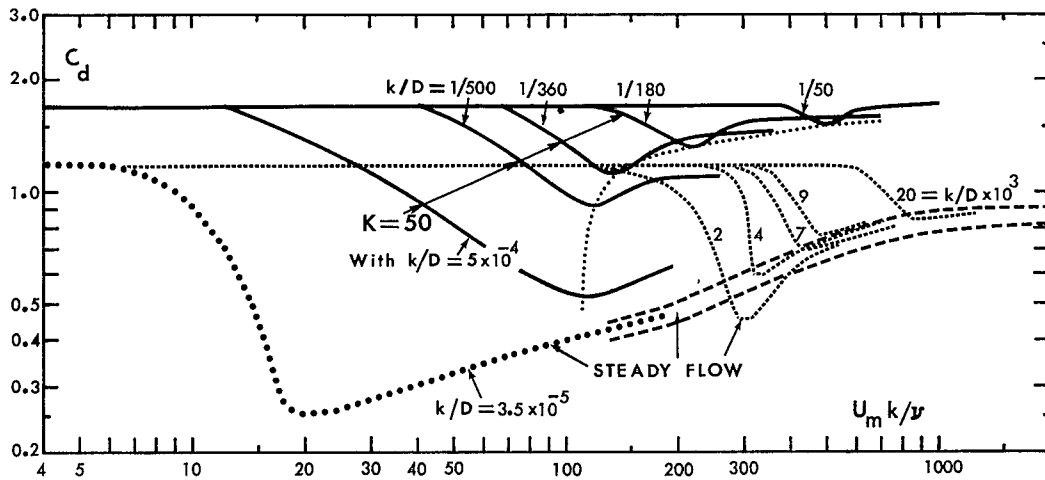
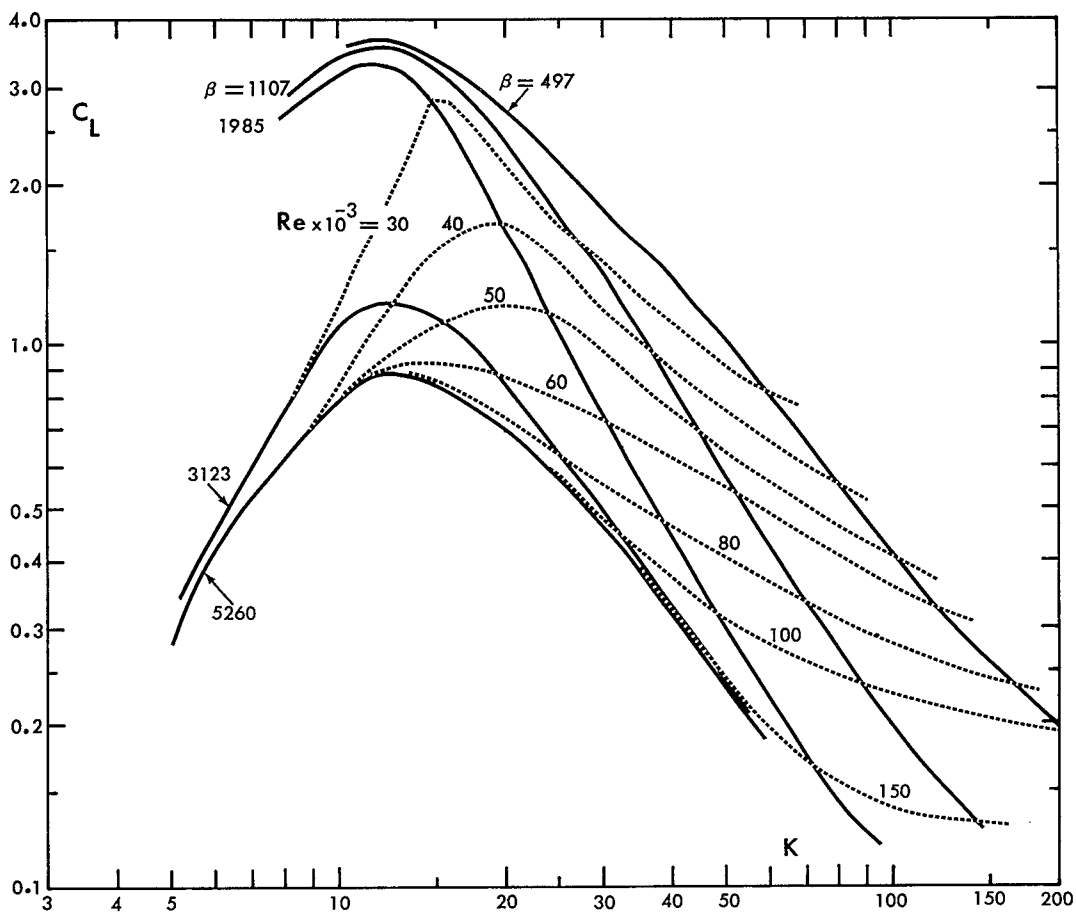FIG. 15 – DRAG COEFFICIENT VS THE ROUGHNESS REYNOLDS NUMBER.

FIG. 16 – LIFT COEFFICIENT VS THE KEULEGAN-CARPENTER NUMBER
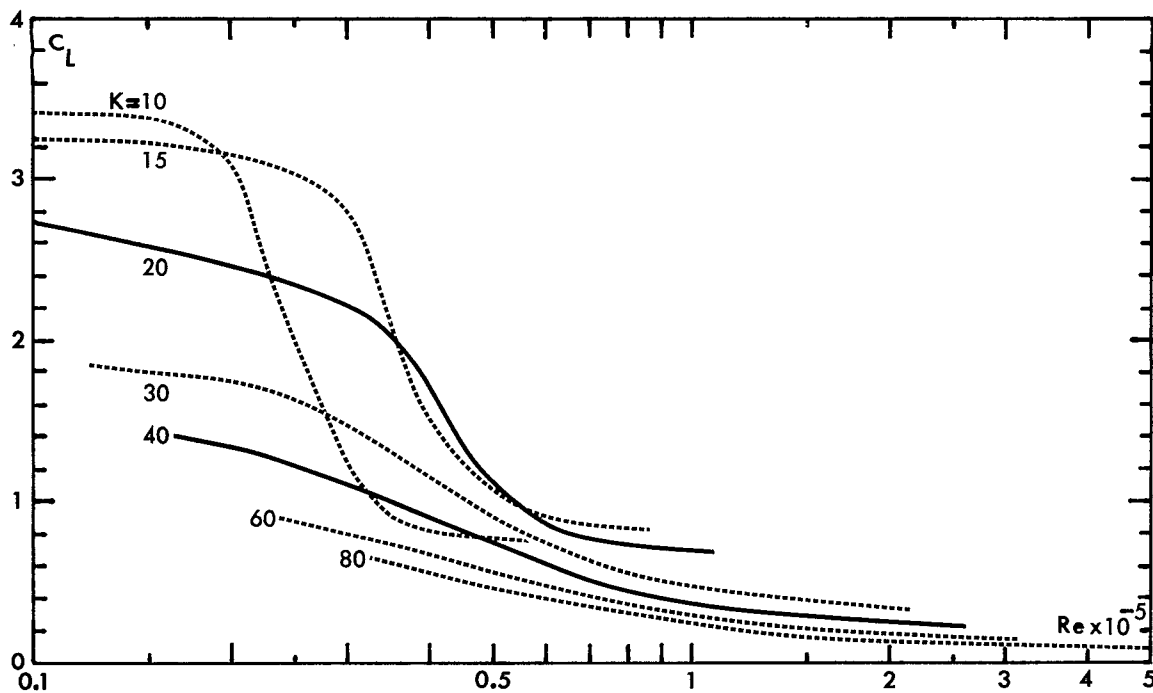FOR CONSTANT VALUES OF THE FREQUENCY PARAMETER AND THE
REYNOLDS NUMBER.

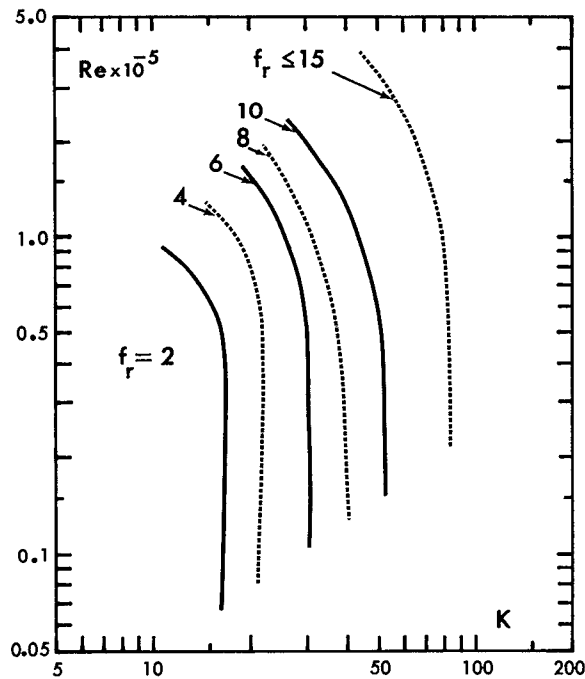FIG. 17 - LIFT COEFFICIENT VS THE REYNOLDS NUMBER FOR CONSTANT VALUES OF K.

FIG. 18 - NORMALIZED VORTEX SHEDDING FREQUENCY AS A FUNCTION OF THE REYNOLDS AND KEULEGAN-CARPENTER NUMBERS.